

Detailed Heat Transfer Investigation Inside a Rectangular Duct with an Array of Ventilated Rib Turbulators

Naveen Sharma, Andallib Tariq and Manish Mishra

Abstract Rib turbulators are extensively studied turbulence promoters employed in numerous industrial applications such as cooling of gas turbine blades and different electronic components, nuclear reactors and compact heat exchangers etc. for heat transfer augmentation. Some of the recent studies have shown the effect of altering rib profiles other than the square along with the effect of slit within it at fixed ratio of rib pitch to height (p/e). The present investigation focuses to explore the effects of p/e ($p/e = 6, 8, 10, 12$) on heat transfer augmentation and pressure penalty. Liquid crystal thermography (LCT) was applied to measure surface temperature distribution with temporal variation and ultimately the local heat transfer coefficients. Transient experiments have been conducted in an open-circuit, suction type air flow system at Reynolds number (Re) ranging from 9400 to 58850 (based on hydraulic diameter of the test section) and at a fixed value of rib height to channel hydraulic diameter ratio (e/D_h) of 0.125. The importance of current work is to appraise the potential impact of rib geometry especially the p/e ratio on the heat transfer enhancement corresponds to square solid and continuous converging slit rib configurations. It is expected, that the experimental data generated from this study will broaden the understanding of heat transfer from fundamental perspective and will serve as a benchmark dataset for validation of computational models.

Keywords Flow control • Friction factor • Heat transfer enhancement • LCT • Rib turbulators

Naveen Sharma (✉) • Andallib Tariq • Manish Mishra
Department of Mechanical and Industrial Engineering, Indian Institute of Technology
Roorkee, Roorkee 247667, India
e-mail: navindme@iitr.ac.in; sharma.naveen28@yahoo.com

Andallib Tariq
e-mail: tariqfme@iitr.ac.in

Manish Mishra
e-mail: mmishfme@iitr.ac.in

1 Introduction

Energy is the essential requirement for globalization, industrialization and to sustain life. Limited availability of conventional energy resources and the environmental deprivation caused by their excessive utilization has necessitated the search for some alternatives to meet the energy requirement for future. Several techniques mainly classified as active, passive and the combined ones have been already proposed towards achieving better heat transfer enhancement [1, 2]. Out of different alternatives, the surface geometry modification such as turbulence promoters is the most effective, economically feasible and rigorously studied. In recent years, the advancement in flow visualization techniques developed new techniques like PIV, LCT, IR, LDV, etc. which permit the measurement of the minute temperature details and also the complete flow field information in a few microseconds [3].

Out of many parameters that influence the performance of duct with rib turbulators, rib installation at optimal position has been acknowledged as the most significant one. Considerable amount of investigations are available in pertinent literature with optical techniques such as infrared thermography (IR) [4, 5] and LCT [6–8] on heat transfer distributions in rectangular ducts with solid rib turbulators. Aliaga et al. [4] reported the presence of separation-reattachment flow distribution at $p/e = 12$ and a trapped vortex flow at $p/e = 5$ between two consecutive ribs. Rau et al. [6] studied the effect of p/e ($p/e = 6, 8, 9, 10, 12, 14$ and 16) on heat transfer characteristics in a duct ($AR = 1$) with ribs mounted on one wall by employing LCT measurement. Maximum heat transfer augmentation is reported at $e/D_h = 0.1$ and p/e of 9 and 12. Wang and Sunden [7] reported superior augmentation heat transfer corresponding to trapezoidal configuration having decreasing height in downstream side of the flow at p/e of 12, e/D_h of 0.1 for Re ranging from 8,000 to 20,000. Tanda [8] reported optimal p/e of 13.33 for one-ribbed and $p/e = 6.66 - 10$ for two-ribbed wall channel corresponding to superior thermal performance.

One of the main problem associated with solid rib turbulators are the formation of hot spots at the upstream and downstream corners, where eddies have been formed which may finally leads to thermal failure in case of gas turbine blades. Thus, the importance of ventilated rib turbulators lies in obviating the formation of such corner eddies or local hot spot. A significant amount of research has been devoted to heat transfer augmentation from a rib roughened surface with different configurations of perforated rib turbulators [9–12] but this is limited to continuous slit ribs [13–19].

Tariq and co-workers have been carried out detailed investigations of heat transfer and fluid flow characteristics in the vicinity of a solid and continuous slit rib [13–17]. It was reported that the optimum open area ratio was 20 % [13]. Further, the reduction in reattachment length (up to 41 %) has been found for inclined split-slit rib when compared with solid rib [18, 19]. The permeable square ribs successfully overpass the establishment of hot spot and significantly reduced the reattachment length by 45 % [20]. Same observations were also made by Ali et al. [15] for trapezoidal rib with continuous slit as compared to solid rib. Furthermore,

the effect of providing a converging slit within a single surface mounted square rib with varying slit converging angles were studied on the basis of PIV and LCT based investigations [16].

The pertinent works offered above shows that most of the investigation was devoted towards the measurement of heat transfer through perforated ribs or through a single rib with continuous slit. There is a shortage of benchmark data on the heat transfer distribution particularly for an array of continuous slit rib configurations. Therefore, an attempt has been made for investigating detailed heat transfer and friction factor characteristics in a channel ($AR = 4:1$) with transversely placed array of solid and continuous converging ventilated ribs on bottom wall using LCT.

2 Experimental Setup and Instrumentation

Transient experiments were performed in an open-circuit, suction type air flow facility developed at Solar and Aerodynamics Laboratory, IIT Roorkee, India. The essential components for LCT measurements are the heating section with liquid crystal sheets and an image acquisition system with lighting arrangement as shown in Fig. 1.

In this open loop air flow facility, room air is drawn through a settling chamber comprising a sequence of honeycomb section, three fine screens, a contraction cone (9:1), and enters at the test section ($AR = 4:1$) due to a suction type blower placed at the end of the flow circuit (Fig. 1). By adjusting the frequency of an A.C. drive panel, the output of blower is controlled and thus the desired required Re is obtained. The heating section (1120 mm \times 184 mm) is designed to satisfy semi-infinite solid model assumption. It comprises of seven composite layers, as described in Fig. 1. Twenty ribs made of Aluminium of square cross section ($e = 8$ mm) having a blockage ratio (e/H) of 0.2, are considered in the present study are depicted in Fig. 1. Array of rib turbulators are placed on TLC coated bottom heated surface of the duct. Investigations with the array of converging slit ribs with converging angle (α) of 15° and an open area ratio (β) of 25 % (downstream-side) have also been performed, and compared with that of square solid ribs.

3 Transient Liquid Crystal Thermography

The experimental approach adopted in the present investigation is similar to that by Ali et al. [15, 17]. For deciding the duration of the actual experiments, first the maximum allowable penetration time for Perspex sheet (12 mm thick) is estimated as proposed by Schultz and Jones [21], which is of the order of 90 s. The total duration of 50 s has been opted for performing actual experiments, which is significantly lower than the maximum permissible penetration time.

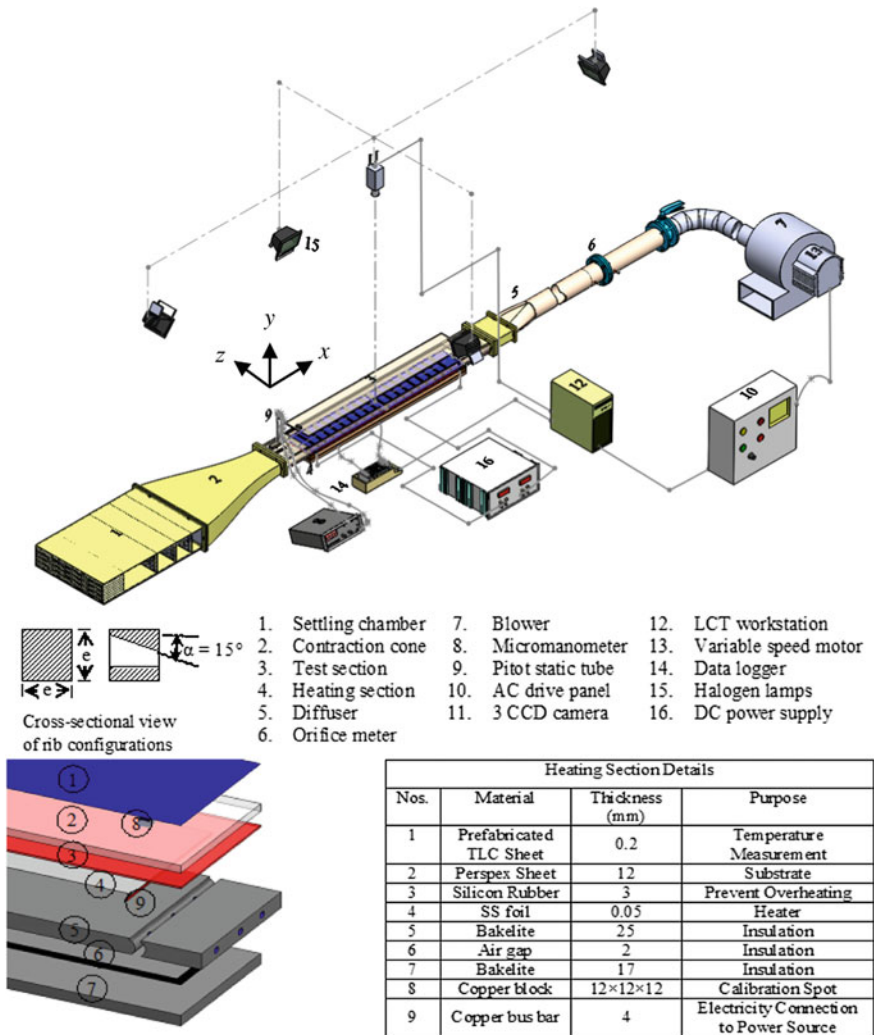


Fig. 1 Schematic of experimental setup for LCT measurements

During experiment, the bottom wall of the test section, which is made up of Perspex and act as the substrate, is heated to a prescribed temperature slightly above the clearing point temperature of the LC sheet. Then, the heated section is exposed to air flow for a step variation in surface temperature. After stabilization of the air flow (<2 s), sequential images of the ROI (region of interest) are captured using 3-CCD video camera for a duration of 50 s with a frame rate of 20 Hz. With the help of 7th order polynomial relationship between hue and temperature obtained from calibration (in situ) experiments, the detailed information regarding surface

temperature distribution at each pixel of the ROI for different time steps has been obtained in terms of temperature matrices.

This temperature information is further processed to calculate the distribution of heat transfer coefficient over the complete heated surface. This can be achieved by solving transient conduction equation in one dimension with an assumption of semi-infinite solid model. The initial (wall temperature) and boundary conditions are applied in Eq. (1) to estimate the distribution of convective heat transfer coefficient over the entire surface.

$$\frac{T_w - T_i}{T_a - T_i} = 1 - \exp\left(\frac{h^2 \tau}{\rho C_p k}\right) \operatorname{erfc}\left(h \sqrt{\frac{\tau}{\rho C_p k}}\right) \quad (1)$$

Here, τ is the actual duration of the complete transient experiment (i.e. 50 s) at which the temperature of TLC-coated surface (at position (x, z)) reaches to a final value (T_w) from the initial surface temperature (T_i) because of the forced flow of air at room temperature (T_a) above the examine surface. h , ρ , and k refer to the convective heat transfer coefficient, density, and thermal conductivity of the Perspex sheet.

4 Results and Discussion

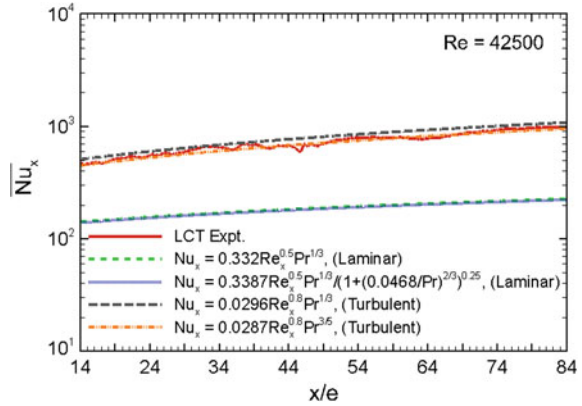
In the present investigation, information regarding the effect of rib geometry (solid and converging slit rib turbulators) and p/e ratios on surface heat transfer distribution and friction factor have been presented for Reynolds number varying from 9400 to 58850. For this purpose, an array (consisting a maximum of 20 ribs) of solid/converging-slit rib with converging angle, $\alpha = 15^\circ$ have been placed transversely on the heated wall of the rectangular duct to cover the entire heating length.

Initially, the span-wise average local Nusselt number ($\overline{Nu}_x = \overline{hx}/k$) variation of the heated surface without rib, along the direction of flow (using transient LCT measurements) has been compared (Fig. 2) with the standard flat plate correlations [22]. Results show a strong agreement at $Re = 42500$ (based on hydraulic diameter) with that of the flat plate correlations for turbulent flows.

For all the experiments with ribbed surface, first rib was placed at fixed position and the position of subsequent ribs has been changed with change in rib spacing. The periodicity in Nusselt number has been observed after 10th, 8th, 7th and 6th rib for p/e equal to 6, 8, 10 and 12, respectively. Acharya et al. [23] and Wang et al. [20] also observed the Nusselt number periodicity well after 6th rib for higher p/e ratios of 20 and 12, respectively.

The comparison of spanwise average augmentation Nusselt number ($\overline{Nu}/\overline{Nu}_0$) distribution for array of solid and converging slit rib turbulators have been shown in Fig. 3, where Nusselt number periodicity has been noticed at different p/e ratios and Re . For solid rib, a tremendously $\overline{Nu}/\overline{Nu}_0$ has been observed in the downstream

Fig. 2 Comparison of Nusselt number correlations [22] for flat plate with experimental data using LCT measurements for smooth surface



vicinity of solid rib, because of low air velocity nearby corner followed by moderate $\overline{Nu}/\overline{Nu}_0$ (after 2 rib height) as a result of flow recirculation and flow reattachment. The rapid rise in Nusselt number is due to emergence of cold air in the direction of bottom surface by the shear layer and further decay of $\overline{Nu}/\overline{Nu}_0$ in downstream direction is because of the growth of new boundary layer. Figure 3 further reveals the mapping of different flow structures such as separation, recirculation and redevelopment for higher p/e ratios ($p/e = 10, 12$) and an immobilized vortex for low p/e ratio ($p/e = 6$). Similar observations are also made by Aliaga et al. [4]. It is noteworthy to point out that there is no redevelopment zone after the reattachment region in case of smaller rib spacing ($p/e \leq 8$). This leads to more uniform distribution of heat transfer augmentation at $p/e = 8$ and 10 than that at $p/e = 12$. Figure 3

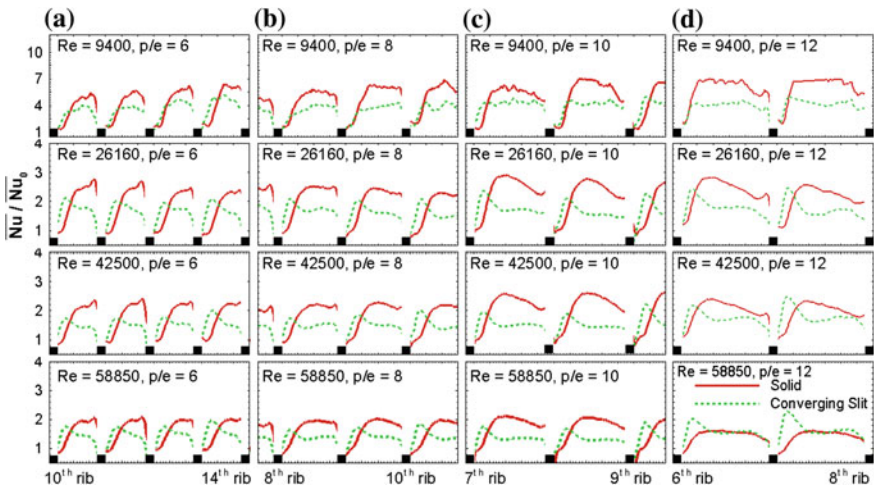


Fig. 3 Spanwise average augmentation Nusselt number distribution for different p/e a 6, b 8, c 10 and d 12 at different Re

also depicts that the increase in p/e ratio shifts the location of maximum heat transfer from nearly $3e$ ($p/e = 6, 8$) to nearly $4e$ ($p/e = 10, 12$) from the rib edge towards downstream region. For higher p/e ratios ($p/e = 10, 12$), next maximum heat transfer rate is witnessed in the vicinity of upstream region of the downstream rib. Similar observation has been reported in Rau et al. [6] and Wang and Sunden [7]. For converging slit rib, $\overline{Nu}/\overline{Nu}_0$ is much higher in downstream region (before 1.8 rib height), but in the region beyond 2 rib height, the array of solid ribs provide superior heat transfer augmentation than array of converging slit ribs. At highest Re and p/e , $\overline{Nu}/\overline{Nu}_0$ is higher for converging slit ribs as compare to solid ribs. Further inspection of Fig. 3, shows the effect of p/e ratios on reattachment length (position of maximum heat transfer augmentation). For both the cases reattachment length shifts towards downstream of the rib as pitch to rib height ratios increases.

Inspection of Table 1 shows that the array of solid ribs gives higher average augmentation Nusselt number ($\overline{(\overline{Nu}/\overline{Nu}_0)}$) as compare to converging slit ribs at all Re and p/e (except at $p/e = 12, Re = 58850$). Maximum value of ($\overline{(\overline{Nu}/\overline{Nu}_0)}$) has been estimated at $p/e = 10$ (except $p/e = 12$ at $Re = 9400$) for solid ribs under turbulent flow conditions; and at $p/e = 12$ for converging slit ribs under the selected range of Reynolds number. Evidently, a completely different flow physics might have attributed towards this change, indicating the need of the present investigation. The pressure penalty observed in terms of friction factor ratio is smaller for array of converging slit ribs than that of solid ribs for all the values of Re and p/e , due to the combined mass and momentum effect into the wake region just downstream of the slitted ribs [14]. The overall thermo-hydraulic performance has been evaluated on the basis of constant pumping power criterion [1, 7–9] and the results have been shown in Table 1. It can be seen that the solid ribs perform better than

Table 1 Performance indexes for different rib configurations at various Re and p/e ratios

	Re	$p/e = 6$		$p/e = 8$		$p/e = 10$		$p/e = 12$	
		Solid	Slit	Solid	Slit	Solid	Slit	Solid	Slit
$\overline{(\overline{Nu}/\overline{Nu}_0)}$	9400	3.65	3.37	4.37	3.06	4.66	3.49	5.53	3.59
	26160	2.22	1.99	2.39	1.88	2.82	1.99	2.79	2.18
	42500	1.67	1.49	1.79	1.39	2.05	1.42	1.89	1.65
	58850	1.53	1.46	1.59	1.29	1.72	1.26	1.43	1.53
(f/f_0)	9400	5.92	4.71	6.83	4.83	6.00	4.58	6.17	4.33
	26160	5.55	4.52	6.43	4.58	5.84	4.35	5.87	4.07
	42500	5.42	4.43	6.28	4.43	5.85	4.20	5.95	3.89
	58850	5.58	4.55	6.44	4.55	6.36	4.27	6.20	3.98
$\frac{\overline{(\overline{Nu}/\overline{Nu}_0)}}{(f/f_0)^{1/3}}$	9400	2.02	2.01	2.30	1.81	2.56	2.10	3.02	2.20
	26160	1.25	1.20	1.29	1.13	1.57	1.22	1.55	1.37
	42500	0.95	0.91	0.97	0.85	1.14	0.88	1.04	1.05
	58850	0.86	0.88	0.85	0.78	0.93	0.78	0.78	0.97

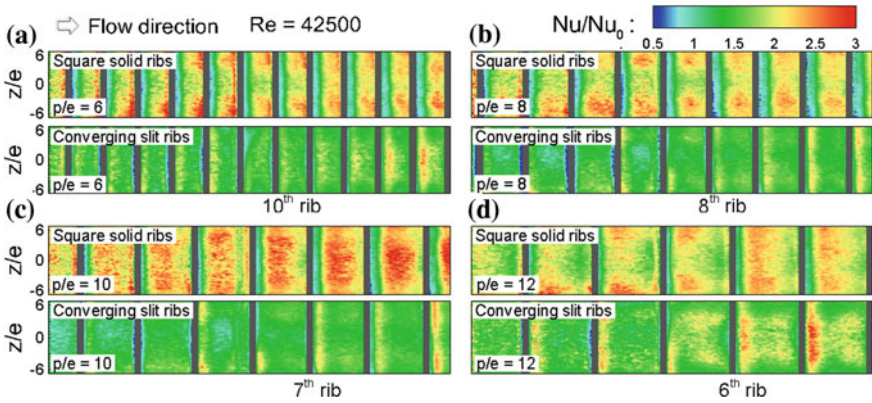


Fig. 4 Mapping of inter-rib local distribution of Nu/Nu_0 for different p/e **a** 6, **b** 8, **c** 10 and **d** 12 at $Re = 42500$

corresponding converging slit ribs for all the investigated ranges of Re and p/e except for $Re \geq 42500$ and $p/e = 12$.

For the sake of brevity, the contours of augmented local Nu/Nu_0 at $Re = 42500$ has been presented (Fig. 4) for region $5.25 \leq x/D_h \leq 14$, due to camera constraints (mainly resolution and coverage area). Rib turbulators are shown by black thick lines on the Nu/Nu_0 contours suggesting their existence only not the value. Figure 4 clearly shows the symmetry of Nu/Nu_0 in spanwise direction for both solid and converging slit ribs. With the introduction of slit, the low velocity region shrinks to a lesser stream-wise distance and a significant reduction in reattachment length is observed. The reason behind this is the jet like flow emerging from the converging slit [14, 18, 19] directly strikes on the surface and causes turbulence mixing just behind the rib. From these results one can easily accept the importance of creating a continuous slit in obviating the formation of local hot spot as observed in case of solid ribs.

5 Conclusion

The local heat transfer distribution and frictional losses over an array of solid and continuous converging slit rib turbulators installed on bottom heated wall of the duct has been estimated. The converging ventilation in the rib yields a jet like flow, which impacts on the wall surface in the leeward corner of the rib causing rigorous mixing of fluid and also cause significant reduction in the reattachment length. As a consequence of this, the higher heat transfer augmentation region shifts towards the rearer corner of the rib. The array of continuous converging slit ribs have been found potentially beneficial in terms of obviating formation of local hot spot by overpassing the corner eddies in the downstream vicinity of the rib as well as in the

upstream corner of the succeeding rib. A significant drop in pressure losses has been observed for converging slit ribs in the form of friction factor as compared to solid rib geometry. The p/e ratios has pronounced impact on augmentation heat transfer and frictional losses. The optimum value of p/e for array of solid and converging slit rib turbulators corresponds to maximum heat transfer enhancement was not same (i.e. $p/e = 10$ for solid ribs and $p/e = 12$ for converging slit ribs). Eventually, the study is found to be useful in understanding of complete temperature and flow field behaviour over the array of surface mounted converging slit ribs.

References

1. Webb, R.L.: Principles of Enhanced Heat Transfer. Wiley, New York (1994)
2. Bergles, A.E.: New frontiers in enhanced heat transfer, in advances in enhanced heat transfer. In: Manglik, R.M., Ravigururijan, T.M., Muley, A., Papar, A.R., Kim, J. (eds.), pp. 1–8. ASME, New York (2000)
3. Camci, C., Glezer, B., Owen, J.M., Pilbrow, R.G., Syson, B.J.: Application of thermochromic liquid crystal to rotating surfaces. *J. Turbomach.* **120**, 100–103 (1998)
4. Aliaga, D.A., Lamb, J.P., Klein, D.E.: Convection heat transfer distributions over plates with square ribs from infrared thermography measurements. *Int. J. Heat Mass transf.* **37**, 363–374 (1994)
5. Gupta, A., SriHarsha, V., Prabhu, S.V., Vedula, R.P.: Local heat transfer distribution in a square channel with 90° continuous, 90° saw tooth profiled and 60° broken ribs. *Exp. Therm. Fluid Sci.* **32**, 997–1010 (2008)
6. Rau, G., Cakan, M., Moeller, D., Arts, T.: The effect of periodic ribs on the local aerodynamic and heat transfer performance of a straight cooling channel. *J. Turbomach.* **120**, 368–375 (1998)
7. Wang, L., Sundén, B.: Experimental investigation of local heat transfer in a square duct with various-shaped ribs. *Heat Mass Transf.* **43**, 759–766 (2007)
8. Tanda, G.: Effect of rib spacing on heat transfer and friction in a rectangular channel with 45° angled rib turbulators on one/two walls. *Int. J. Heat Mass Transf.* **54**, 1081–1090 (2011)
9. Hwang, J.J., Liou, T.M.: Heat transfer augmentation in a rectangular channel with slit rib-turbulators on two opposite walls. *J. Turbomach.* **119**, 617–623 (1997)
10. Hwang, J.J.: Heat transfer-friction characteristic comparison in rectangular ducts with slit and solid ribs mounted on one wall. *J. Heat Transf.* **120**, 709–716 (1998)
11. Liou, T.M., Chen, S.H., Shih, K.C.: Numerical simulation of turbulent flow field and heat transfer in a two-dimensional channel with periodic slit ribs. *Int. J. Heat Mass Transf.* **45**, 4493–4505 (2002)
12. Nuntadusit, C., Wae-hayee, M., Bunyajitradulya, A., Eiamsa-ard, S.: Thermal visualization on surface with a transverse perforated rib. *Int. Commun. Heat Mass Transf.* **39**, 634–639 (2012)
13. Panigrahi, P.K., Tariq, A.: Liquid crystal heat transfer measurements in a rectangular channel with solid and Slit rib. *J. Vis.* **6**, 407–416 (2003)
14. Tariq, A., Panigrahi, P.K., Muralidhar, K.: Flow and heat transfer in the wake of a surface mounted rib with a slit. *Exp. Fluids* **37**, 701–719 (2004)
15. Ali, M.S., Tariq, A., Gandhi, B.K.: LCT and PIV investigations behind trapezoidal-rib with a slit mounted on bottom wall of a rectangular duct. In: Proceedings of ASME 2012 Gas Turbine India Conference, pp. 313–325, ASME (2012)
16. Ali M.D.: Fluid flow and heat transfer investigations behind surface mounted solid and slitted ribs. PhD Thesis, MIED, IIT Roorkee (2012)

17. Ali, M.S., Tariq, A., Gandhi, B.K.: Flow and heat transfer investigation behind trapezoidal rib using PIV and LCT measurements. *Exp. Fluids* **54**(1520), 1–15 (2013)
18. Panigrahi, P.K., Schroeder, A., Kompenhans, J.: PIV investigation of flow behind surface mounted permeable ribs. *Exp. Fluids* **40**, 277–300 (2006)
19. Panigrahi, P.K., Schroeder, A., Kompenhans, J.: Turbulent structures and budgets behind permeable ribs. *Exp. Therm. Fluid Sci.* **32**, 1011–1033 (2008)
20. Sunden, B.: Convective heat transfer and fluid flow physics in some ribbed ducts using liquid crystal thermography and PIV measuring techniques. *Heat Mass Transf.* **47**, 899–910 (2011)
21. Schultz, D.L., Jones, T.V.: Heat Transfer Measurements in Short Duration Hypersonic Facilities. Technical Report, NATO Advisory Group Aeronautical RD (1973)
22. Kays, W.M., Crawford, M.E.: *Convective Heat and Mass Transfer*, 3rd edn. McGraw-Hill Inc., United States of America (1993)
23. Acharya, S., Dutta, S., Myrum, T.A., Baker, R.S.: Periodically developed flow and heat transfer in a ribbed duct. *Int. J. Heat Mass Transf.* **36**, 2069–2082 (1993)